

Original Article

# Development of Unique Cowrie Shell Inspired 3D Printed Cufflinks

B. Ambika<sup>1</sup>, Yeole Shivraj Narayan<sup>1\*</sup>, Kode Jaya Prakash<sup>1</sup>

<sup>1</sup>Mechanical Engineering, VNR Vignana Jyothi Institute of Engineering and Technology, Hyderabad, Telangana, India.

\*Corresponding Author : [shivrajyeole@vnrvjiet.in](mailto:shivrajyeole@vnrvjiet.in)

Received: 08 July 2024

Revised: 11 August 2024

Accepted: 10 September 2024

Published: 30 September 2024

**Abstract** - Jewellery design is a profession that involves creating intricate jewellery, but it is a time-consuming and complex manufacturing method. Conventional jewellery manufacturing involves labour, complex designs, skilled craftsmen, patience, and time, leading to increased waste generation. To stay relevant in a dynamic market, traditional jewellery manufacturers need unique and appealing designs, precise measurements, high-quality materials, prompt delivery, and waste management. This work is aimed at demonstrating the utility of 3D printing in creating unique and novel nature-inspired cufflink designs to mitigate the issues mentioned above. 3D printing aids in fulfilling customer expectations providing solutions to product complexity, cost-effectiveness, and time efficiency. It maintains effective customization by modelling intricate designs through CAD, thereby overcoming the challenges. The process involves selecting a nature-inspired design form for cufflink jewellery using the Quality Function Deployment (QFD) tool. Cowrie shell is finalized as the nature-inspired form for the design of cufflink using QFD outcomes. Three cowrie shell cufflink conceptual models with oval, cross, and hexagonal base structures are created and converted to CAD models via 3D scanning and CAD modelling. These designs are then subjected to tensile and compressive loading ranging from 19.6 N to 100 N on PLA and castable wax resin materials for maximum stress and displacement. Tensile and compressive analysis results indicate that castable wax resin material has a higher von-Mises stress but is within the limit as compared to that of PLA material. Wax materials exhibited more displacement than PLA materials. Hence, cowrie shell-inspired cufflink models are then 3D printed using castable wax resin material on an SLA printer. Unique nature-inspired, i.e., cowrie shell cufflinks, are successfully obtained using the SLA 3D printing technique.

**Keywords** - 3D printing, SLA printing, Jewellery, Cufflink, Cowrie shell, Nature inspired.

## 1. Introduction

Jewellery is a personal or familial heirloom that can have a variety of characteristics and purposes. It may be a sentimental object handed down through the years or a family heirloom. Jewellery is a symbolic item of various uses, often passed down through generations. It serves as money, demonstrates or stores value, and is valued as a valuable asset. Understanding its symbolism and meanings is challenging due to its context, materiality, and creator/user [1, 2]. Jewellery is a well-liked aesthetic item that has elegant, recognizable elements [3]. Indian societies have used jewellery for social rituals, and designs often reflect devotion to the sun, moon, and snake. Charms for good fortune were popular, while marriage symbols represented troth, indicating regional differences in cultural value [4]. Jewellery design started in the early Paleolithic and became a useful craft for man-made beauty accessories in the Renaissance [5]. Jewellery designers utilize inspiration, idea generation, and product assessment to create wearable jewellery, but comprehending their thinking and knowledge development is challenging due to interconnected design and

manufacturing processes [1]. Since ancient times, jewellery has been used to enhance physical beauty. From hairpins to toe rings, many kinds of jewellery adorn every aspect of the human body [6].

### 1.1. Cufflinks

Cufflinks are jewellery pieces that fasten the cuffs of dress shirts. They come in a variety of materials. Toggles, reverse chains, or a stiff rear part can be used to secure them [7]. Since the end of the 18th century, cufflinks have gained popularity as a fashionable ornament. Men also started adding frills, ruffs, and cufflinks to the exposed areas of their shirts following the Middle Ages. Originally, people wore collared tunics with sleeves [8]. Various types of cufflinks are available in the market, like bullet back cufflink, whale cufflink, fixed back cufflink, ball return cufflink, chain style cufflink, locking cufflink, knot cufflink, stud cufflink, and fabric cufflink [9].

### 1.2. 3D Printing

Additive Manufacturing (AM) is a rapidly evolving field that aims to revolutionize manufacturing by combining



materials to create items from 3D mathematical models [10]. The ASTM F42 Committee defines AM as a procedure of fusing material to create objects from 3D model data layer by layer [6]. Three-dimensional printing is a consumer-focused technology that produces 3D models from a layer of materials and has many applications in the aerospace, medical, engineering, construction, automotive, and architectural industries [11]. It is a process that uses selective materials deposited through a nozzle to produce items. Additive techniques are utilized to manufacture goods from CAD data [12]. AM utilizes Computer Design files (CAD) to create intricate structures from liquid molecules or powder grains [13], with surface geometry data stored in STL files for jewellery models [11]. 3D printing technology helps jewellery designers fulfill consumer expectations for unique and personalized things [14].

### 1.3. Inspired Design

Jewellery has been used as a traditional art form. It is usually made from natural materials such as seeds, flowers, feathers, leaves, claws, animal bones, stone beads, bones, and wood [15]. Function, design, and aesthetics are the main emphasis of nature-inspired designs, which aids in problem-solving and creative thinking. It is essential to both inanimate objects and biological systems [16]. Design is inspired by the variety of forms, structures, shapes, colours, textures, and materials found in nature. The elements of nature have been adapted by humans and created into distinctive jewellery with a unique sense of symbolism and history [17]. The initial themes in jewellery, a universal decoration type, were flowers and floral designs. Jewellery was first made from prehistoric shells and stone [18]. Some examples of jewellery include bracelets, cufflinks, earrings, necklaces, brooches, and rings.

#### 1.3.1. Literature Review

The utility of 3D modelling has been utilized in artisanal jewellery production, highlighting its potential to blend contemporary manufacturing methods with traditional techniques. Cultural and moral aspects of authenticity in craft provide a counterpoint to mass-produced society, highlighting the innovative possibilities and efficiencies of 3D modelling technology. The study emphasized the importance of preserving the human touch in the craft industry [2]. A study on 3D printing precious metals for jewellery manufacturing using Direct Metal Laser Sintering (DMLS) was conducted to create four rings from titanium, gold, silver, and stainless steel 316L. The equipment was found to be efficient and had less metal powder. Examination of metals through an electron microscope revealed differences between titanium and gold and stainless steel and silver. DMLS technology offers a competitive option for the jewellery industry [14]. Master's students from the University of Ljubljana transformed wooden sculptures into 3D-printed jewellery, focusing on innovative production, business, marketing, fashion accessories, 3D print design, and theoretical foundations. The project showcased nearly

130 pieces of oak wood sculptures at Forma Vivas Open Air Wood Series [19]. The utility of statistical methods in 3D printing for design and testing optimization, focusing on the Taguchi methodology, Weibull analysis, and factorial design, has been presented in a study by Espino and Michaela T et al. [20]. The study suggests that these tools are essential for optimizing mechanical properties in 3D printing [20]. AM techniques were explored in creating jewellery and clothing for the fashion industry with a focus on the benefits of design freedom and complex patterns, as well as the data capture, modelling, software, and post-processing techniques involved [21]. Achieving sustainability through AM in fashion design is also another notable research. Softwares like Rhinoceros5 and Tinker CAD are used along with MakerBot Replicator 2 and Polylactic acid filaments. The method promotes zero-waste principles by creating intricate designs through successive material layers. The research aims to create sustainable and innovative designs that promote zero-waste principles [22]. A comparative investigation of AM, specifically DMLS, with a conventional technique like investment casting for the jewellery sector has been presented by Ferreira and Telma et al. [23]. DMLS is more effective and requires less heat, backing material, and cleaning. The study also used a computational program for online evaluation and step-by-step modification of the design, enhancing the efficiency of the process [23]. Sintering technologies and powder metallurgy are disrupting the global jewellery manufacturing sector in design and manufacturing. The research also explores Ojo technology's potential cost savings and design versatility [24].

Inspired jewellery is the art of creating wearables from inspiration, combining creative methods, precision, and attention to detail to create meaningful and stunning pieces that convey a message or feeling, transcending ornamental components to capture the designer's vision. Nature has been inspiring human creativity and problem-solving, leading to the development of design strategies that combine historical sources, rhythms, sounds, constellations, and themes to create models that emphasize design, function, and nature's beauty [16]. The beauty and components of the natural world serve as inspiration for nature-inspired jewellery, which frequently features leaves, flowers, animals, and other natural shapes. Traditional jewellery manufacturing is labour-intensive, complex, and time-consuming, leading to customized products and increased waste. Manufacturers need precise measurements, high-quality materials, and prompt delivery to remain competitive [25]. Traditional manufacturing methods also result in more waste production and difficulty in creating unique, intricate designs, as designers often struggle to create appealing designs [26]. This work is aimed at creating novel nature-inspired jewellery designs that could be additively manufactured. The work focuses on the modelling, analysis, and fabrication of a novel cowrie shell-inspired cufflink using additive manufacturing.

## 2. Materials and Methods

Industrial 3D printers may use Fused Deposition Modelling (FDM), Selective Laser Sintering (SLS), and polyjet printing processes to print materials like bronze, gold, and stainless steel. Because polymer composites are adaptable and not heavy, they are suited for 3D-printed jewellery [21]. AM technologies like SLA use high-performance resins and waxes to build models, prototypes, gadgets, and products from a variety of materials. For jewellery prototypes, resins are essential for replicating precise settings, clear jaws, elegant stems, and high-quality surface details, while wax is recommended for intricately shaped moulds [10-13]. Powder Bed Fusion (PBF) is a 3D printing technique used in jewellery production to create high-quality items out of materials, including wood, nylon, acrylonitrile, and polycarbonate [14]. 3D printers use virgin materials like weave textiles, such as PLA, ABS, and flexible filaments. PLA is recommended because of its better stability, lower melting point, and biodegradability [22]. Titanium (Ti) is a versatile material that, because of its mechanical resistance, biocompatibility, colour, brightness, and endless colour manufacturing possibilities, is frequently employed in the jewellery and biomedical areas [27]. PLA and Castable Wax Resin are commonly used in jewellery making due to their ease of 3D printing, quick prototyping, biodegradability, and diverse colour options. PLA is popular in various applications because of these qualities. On the other hand, the accuracy and ability to capture fine details of Castable wax resin make it a popular material for jewellery manufacturing. It works well with various casting methods and metals, making it a dependable option for jewellers. Figure 1 depicts the methodology adopted for executing the work. This involves choosing a nature-inspired form for jewellery ornament, developing conceptual designs, creating models using CAD software, and then analysing them for different loads using analysis software. The findings from this analysis will determine the 3D printing process for the jewellery ornaments.

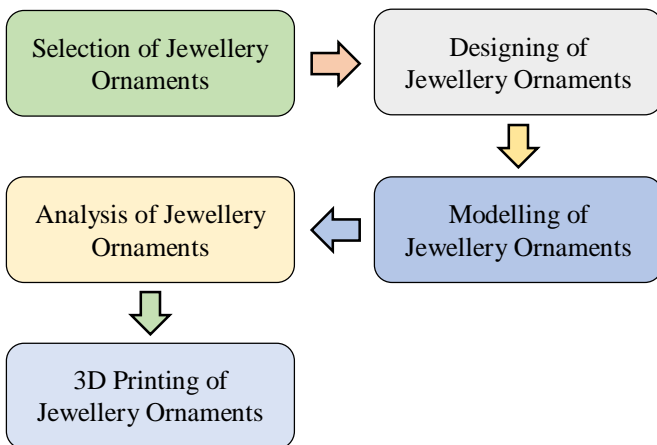


Fig. 1 Step-wise process flow

### 2.1. Selection of Jewellery Ornament

This research aimed to create wearable designs inspired by nature. However, there are plenty of sources in nature to look for, like sculptures, flowers, etc. Through a literature review, sea shells, flowers, fruits, and plants were selected as possible candidates for evaluation. Quality Function Deployment (QFD) tool is used to finalize the inspired form. Based on the outcomes of the QFD approach, the nature-inspired form is selected for the design of the cufflink. Table 1 illustrates the parameters used to choose the nature-inspired design.

Table 1. Selection criteria

Criteria	✓	☑	✗
Availability of the inspired item	Readily Available	Medium	Not Available
Shape/form of the inspired item	Complex	Moderate	Easy
Cost of the inspired item	Cheap	Moderate	Expensive
Size of the inspired item	Small	Medium	Large

Nature-inspired forms such as sea shells, flowers, fruits, and plants are assessed using Quality Function Deployment (QFD). The selection of nature-inspired form is made based on the desired parameters, including market availability (readily available), complex shape, low cost, and small size. The outcomes are depicted in Appendix 1 and 2. Cowrie shell is selected as the nature-inspired form for the cufflink jewellery design. Figure 2 exhibits the natural cowrie shell. After reviewing the literature on cufflinks, it was found that cufflinks are traditionally manufactured using metal materials. The use of a cowrie shell-inspired form on a cufflink via AM is the novelty of the work. As a result, it was decided to create the cufflinks using an SLA 3D printing process with castable wax resin material.



Fig. 2 Cowrie shell

**2.2. Conceptual Design**

This study focuses on the design of nature-inspired jewellery, particularly cufflinks, which may be produced primarily with the use of 3D printers for concept development. The initial design process involves creating a conceptual model of cufflink. Three conceptual designs, i.e., Design 1 consisting of a square shaft and oval base, Design 2 consisting of a round shaft and cross base, and Design 3 consisting of a hexagonal shaft and hexagonal base, are sketched as shown in Figure 3. A cufflink generally consists of a base, a shaft, and a top platform. The inspired form of the cowrie shell is placed over the top platform in the conceptual designs.

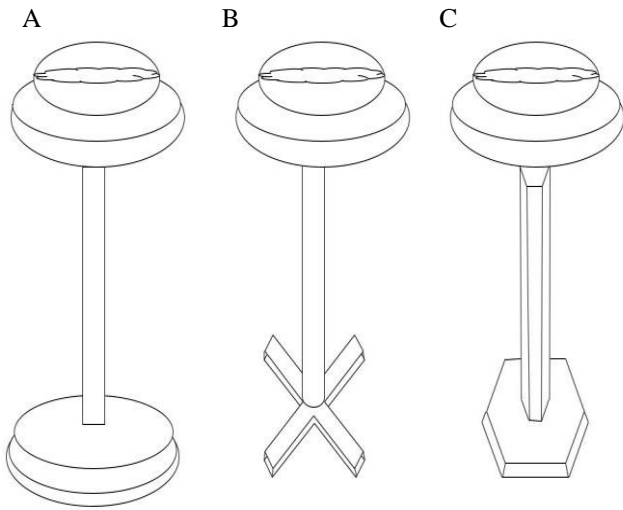


Fig. 3 Conceptual designs of cufflinks. (A) Design 1, (B) Design 2, and (C) Design 3.

**2.3. Design of Cowrie Shell-Inspired Cufflink**

Modelling of a nature-inspired cufflink is carried out in two steps. The first step is the modelling of the cowrie shell, and the second step is the modelling of the cufflink.

**2.3.1. Modelling of Cowrie Shell**

The cowrie shell is modelled through the reverse engineering process. It begins by gaining dimensional information about the object via 3D scanning. In reverse engineering, the 3D scanning method includes creating application-specific geometric models, point processing, and scanning. The process of creating a point cloud and CAD model from an object is shown in Figure 4 [28].

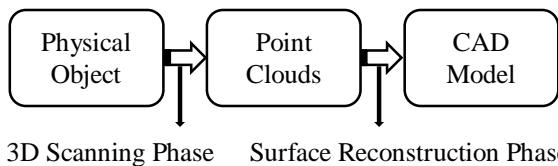


Fig. 4 Reverse engineering process using 3D scanning technique

For the reverse engineering process, a Zeiss 3D scanner, specifically the COMET L3D25M with blue light technology, is used to obtain detailed and accurate 3D meshes. The scanning and calibration process took approximately 1 hour and 40 minutes. Figure 5(A) demonstrates different views of a scanned cowrie shell model. Once the 3D point cloud data file is achieved, then the STL file is generated, which is used for modelling nature-inspired cowrie shells in the Autodesk Fusion 360 v2.0 software. Figure 5(B) shows the model of a sliced cowrie shell resting on the platform of the cufflink.

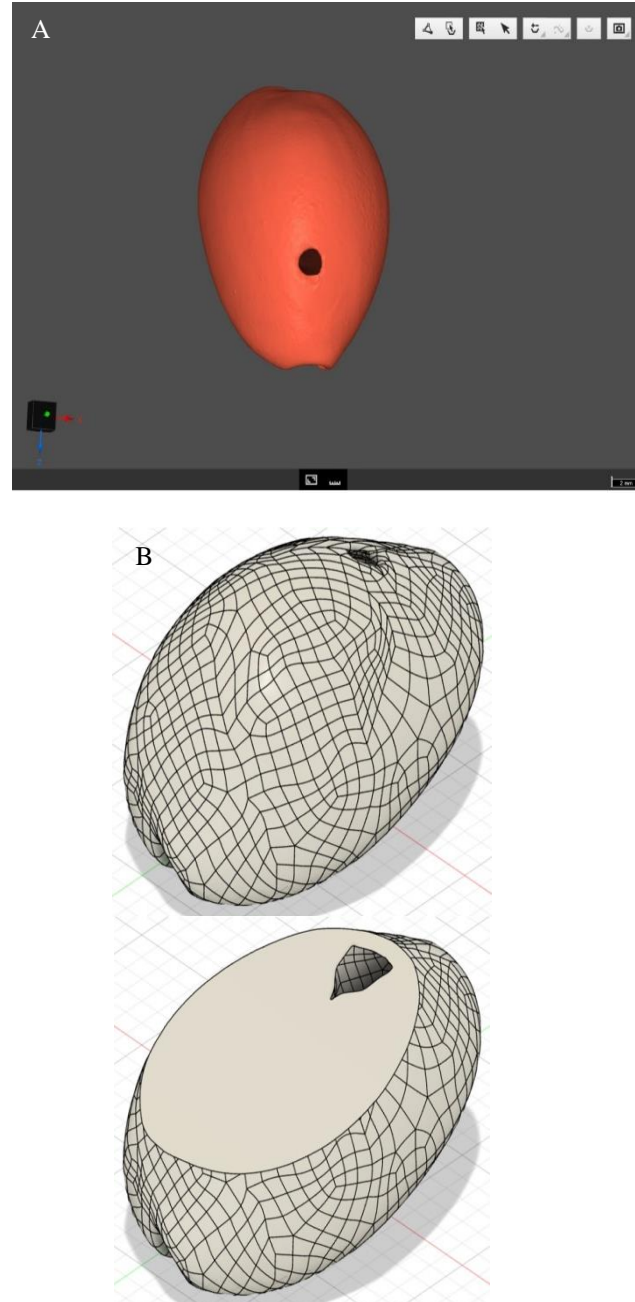


Fig. 5 Cowrie shell modelling (A) Scanned cowrie shell, and (B) Sliced cowrie shell.



### 2.3.2. Modelling of Cufflink

Figure 6 displays a standard commercial cufflink. The dimensions of this cufflink are used as the reference dimensions for modelling the cufflink. Dimensions are measured using digital vernier calipers. The platform has dimensions of 18 mm x 3 mm, the shaft has dimensions of 16.55 mm x 2.39 mm x 2.62 mm, and the base part has dimensions of 17.65 mm x 7.6 mm x 2.2 mm. Autodesk Fusion 360 v2.0 software is employed in the base modelling of the Cufflink. Figure 7 exhibits the cufflink models with different bases.



Fig. 6 A standard cufflink

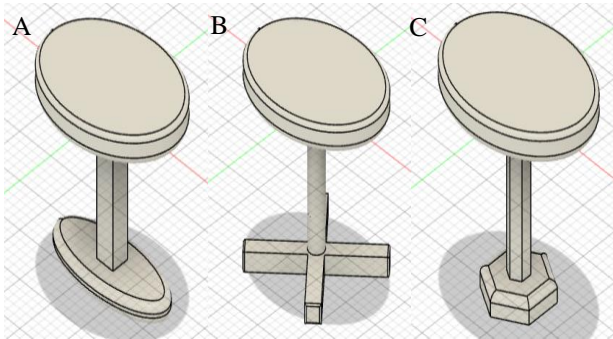


Fig. 7 Cufflink models. (A) Oval base, (B) Cross base, and (C) Hexagonal base.

The final cufflink model is formed using the cufflink base and nature-inspired cowrie shell form and saved in .stl format for further processing. Figure 8 displays the three-cowrie shell-inspired cufflink designs modelled based on conceptual design.

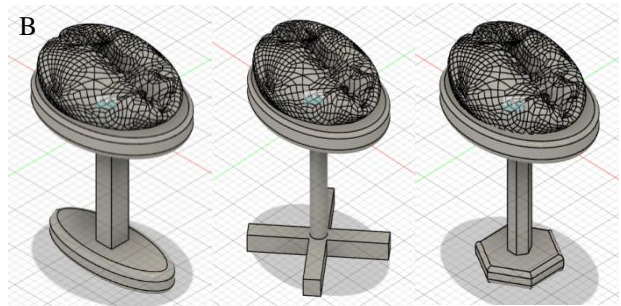
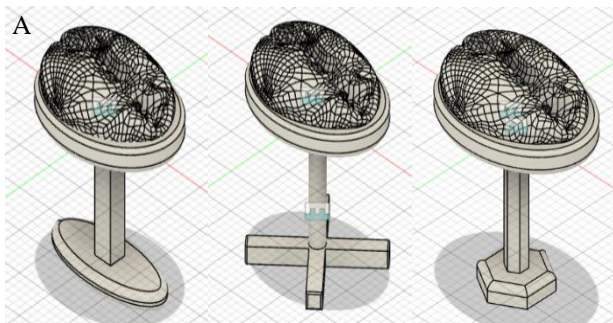


Fig. 8 Cowrie shell-inspired cufflinks models (A) With PLA, and (B) With castable wax resin.

### 2.4. Analysis of Cowrie Shell-Inspired Cufflink

The CAD designs are then subjected to simulation using Autodesk Fusion360 v2.0 software. Tensile and compressive strength analysis is conducted using Polylactic Acid (PLA) and castable wax resin materials, with fixed support at the cufflink base and load of 19.6 N, 25 N, 50 N, 75 N, and 100 N, respectively applied on the top of the cufflink. This study analyzed the model's total deformation and maximum stress using the finite element method to comprehend the model's behavior under specific load conditions. Figure 9 illustrates the boundary conditions applied on the cowrie shell-inspired cufflink.

The parameters considered in the analysis are,  
 $\sigma$  = von-Mises Stress (MPa)  
 F.S = Factor of safety and  
 S = Displacement (mm)

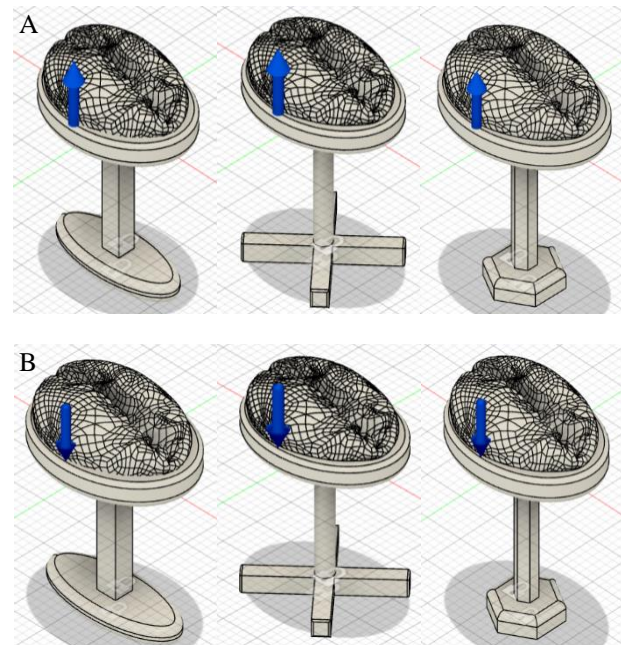


Fig. 9 Boundary conditions applied on the Cufflink Designs. (A) Tensile force is applied to cufflink designs, and (B) Compressive force is applied to cufflink designs.

**2.5. Design for 3D Printing of Cowrie Shell-Inspired Cufflink**

It is essential to verify that a 3D model is error-free before printing, as most CAD programs generate STL files with minor mistakes. Point-to-point capture with 3D scanners is used for repair, and slicing software divides the model into small layers. After the CAD model has been translated to STL format and loaded with consumables, the printer sets settings and begins layer-by-layer construction of the object, which may take several hours [29, 30].

The STL file of the cowrie shell model can be opened only with specific CAD software. STL file is processed into the CATPart file extension, which is subsequently opened in Autodesk Fusion 360 v2.0 software. The imported file is used to modify and create a total cufflink model. Pre-repairing and optimization of the mesh are accomplished using relevant tools. For 3D printing, model files are imported into Chitubox V1.9.6 software, and the process is performed after building support structures on the cufflink model.

Colin 3D software is utilized for editing and removing noise errors surrounding the cowrie shell, as depicted in Figures 10(A) and 10(B). The STL file is then exported without any errors, as shown in Figure 10(C).

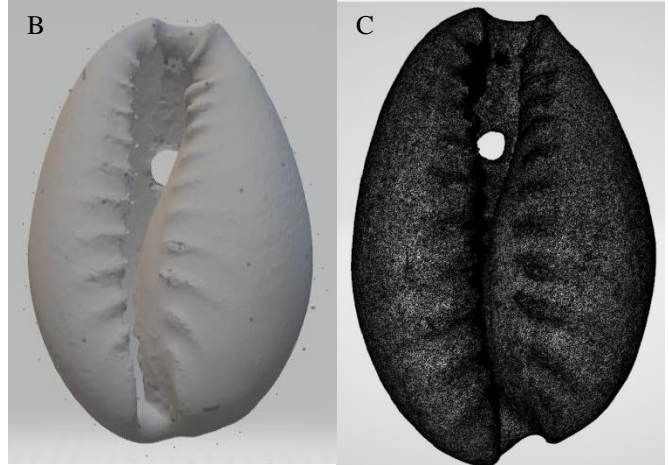


**Fig. 10** Error rectification (A) Noise at cowrie shell, (B) Removal of noise errors, and (C) Exported STL file.

**3. Results and Discussion**

**3.1. Modelling and Analysis of Cowrie Shell-Inspired Cufflink**

A detailed analysis of the CAD model cufflink designs is executed, and the results are presented in the subsequent tables and graphs, as well as in Appendix 3. Appendices 3.1, 3.2, and 3.3 present the analysis results of tensile and compressive tests carried out on Design 1 (Oval base), Design 2 (Cross base), and Design 3 (Hexagonal base), respectively.

Table 2 and Figure 11 show the changes in von-Mises stress and displacement for Design 1 under increasing tensile load from 19.6 N to 100 N.

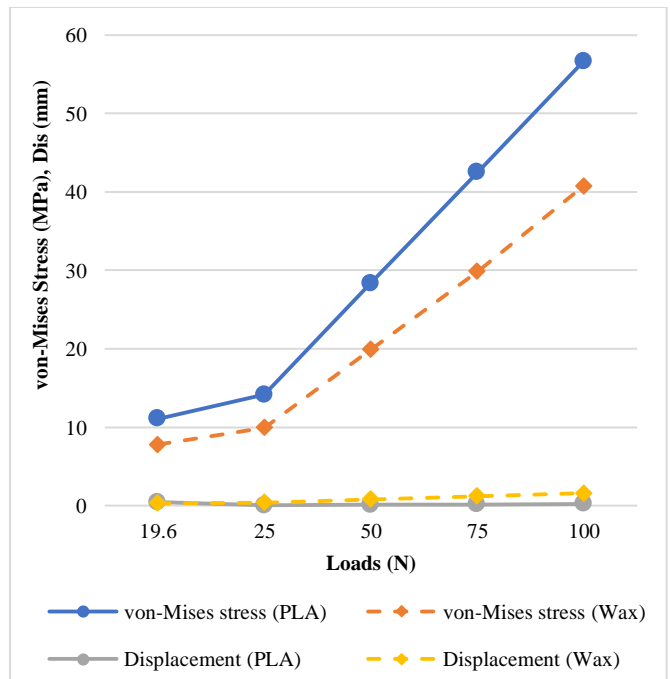
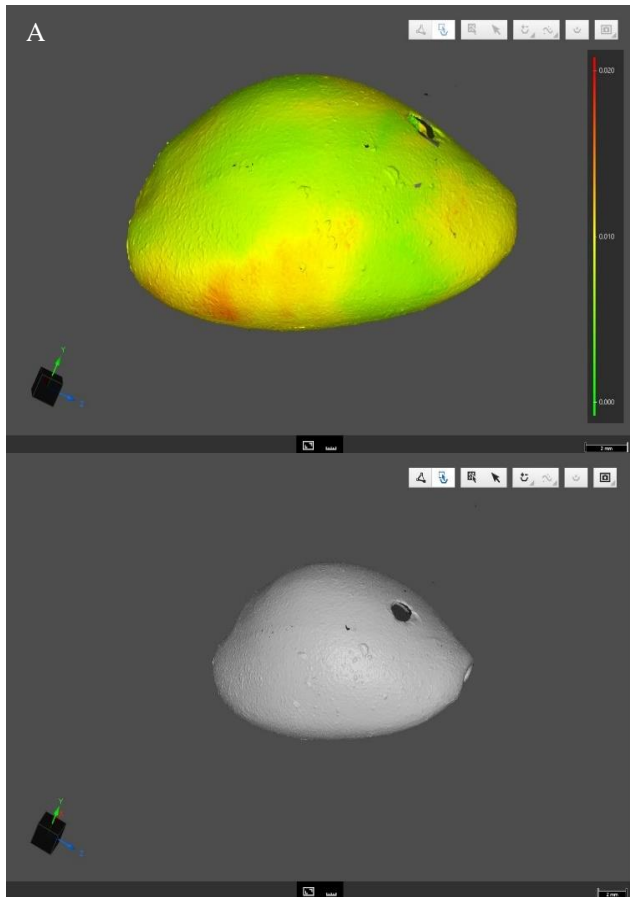


**Fig. 11** Von-mises stress and displacement vs Tensile load for Design 1

**Table 2. Tensile strength analysis on design 1**

Loads (N)	von-Mises stress (MPa)		Displacement (mm)	
	PLA	Wax	PLA	Wax
19.6	11.106	7.806	0.44	0.315
25	14.166	9.957	0.056	0.402
50	28.332	19.913	0.112	0.803
75	42.498	29.87	0.168	1.205
100	56.664	40.755	0.224	1.602

As seen in Figure 11, the PLA and wax material models show a proportional increase in stress with increasing tensile load. The maximum equivalent von-Mises stress at 100 N load is 56.664 MPa for PLA and 40.755 MPa for castable wax resin. The analysis indicates potential breakage in the PLA material at 100 N load, with no breakage for the wax resin material under the given loads. However, it is worth considering further wax processing due to its proportional increase in stress with the load, resulting in a more predictable and consistent stress response. The displacement in PLA material is minimal (decreasing minimally) with increasing load.

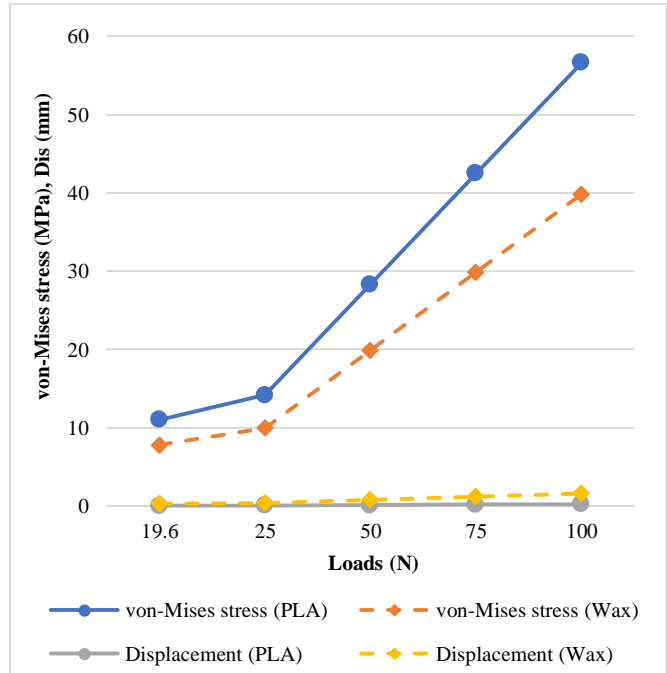
On the other hand, displacement is found to increase with increasing load for castable wax resin. This difference suggests that the PLA material exhibits a potential stiffening effect or resistance to deformation. In contrast, the castable wax material shows greater pliability and deformation under stress, as evidenced by the increasing displacement values with higher loads. These contrasting behaviors under increasing load conditions indicate significant material differences. When a tensile load is applied to the model, the castable wax resin material has an adequate von-Mises stress and displacement in contrast to the PLA material.

Table 3 and Figure 12 show the changes in von-Mises stress and displacement for Design 1 under increasing compressive load from 19.6 N to 100 N. The PLA and the castable wax resin materials showed a consistent stress response. The maximum equivalent von-Mises stress at 100 N load is 56.662 MPa for PLA and 39.825 MPa for castable wax resin. This implies that the wax material can endure higher stress levels than PLA under the same loading conditions because it will fail under 100 N load conditions, exceeding its yield strength.

The displacement in PLA and wax materials exhibits a clear trend, where the displacement values increase with the applied load. At a load of 100 N, both materials show a maximum displacement, while at a 19.6 N load, they exhibit minimum displacement. When a compressive load is applied, the PLA material shows a higher maximum von-Mises stress than the wax material. In terms of displacement, the wax material exhibits more deformation than the PLA material model.

**Table 3. Compressive strength analysis on design 1**

Loads (N)	von-Mises stress (MPa)		Displacement (mm)	
	PLA	Wax	PLA	Wax
19.6	11.04	7.805	0.044	0.315
25	14.164	9.955	0.056	0.402
50	28.329	19.912	0.112	0.803
75	42.496	29.869	0.168	1.205
100	56.662	39.825	0.224	1.606



**Fig. 12 Von-mises stress and displacement vs Compressive load for design 1**

**Table 4. Tensile strength analysis on design 2**

Loads (N)	von-Mises stress (MPa)		Displacement (mm)	
	PLA	Wax	PLA	Wax
19.6	10.204	17.694	0.034	0.475
25	13.015	17.521	0.043	0.601
50	26.03	43.658	0.087	1.193
75	39.045	67.835	0.13	1.797
100	52.061	70.087	0.17	2.403

Table 4 and Figure 13 illustrate the changes in von-Mises stress and displacement for Design 2 under increasing tensile load from 19.6 N to 100 N. A gradual increase in stress, showing a proportional rise in stress relative to the applied load, is seen in PLA material. In contrast, castable wax resin material demonstrated an increase in stress beyond 25 N load. The maximum equivalent von-Mises stress at 100 N load is 52.061 MPa for PLA and 70.087 MPa for castable wax resin, indicating that the stress level in the wax material is significantly higher than the PLA material. This underscores the greater



stress endurance capacity of wax under the same loading conditions. The relationship between load and resulting stress clearly illustrates the distinct mechanical properties and performance of PLA and wax materials under load. The displacement in PLA and wax materials both exhibit an increase in displacement values with increasing load. This behavior highlights that both materials deform more significantly under higher loads, with maximum displacement observed at 100 N and minimum displacement at 19.6 N. When a tensile load is applied, the castable wax material has maximum von-Mises stress and displacement in contrast to the PLA material.

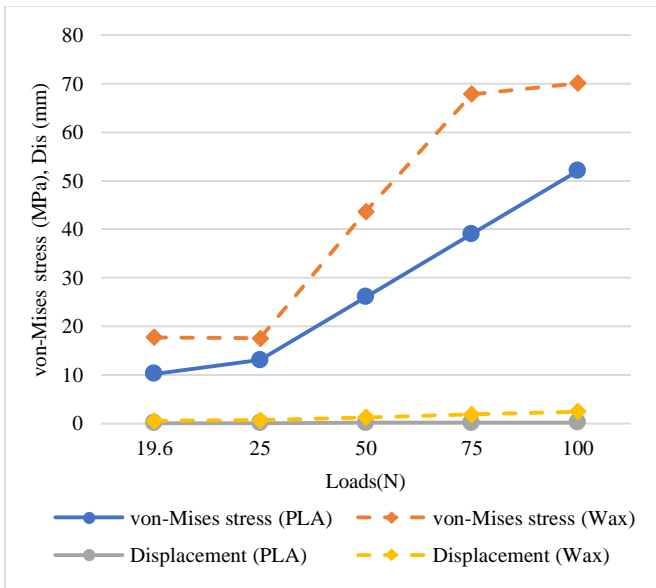


Fig. 13 Von-mises stress and displacement vs Tensile load for Design 2

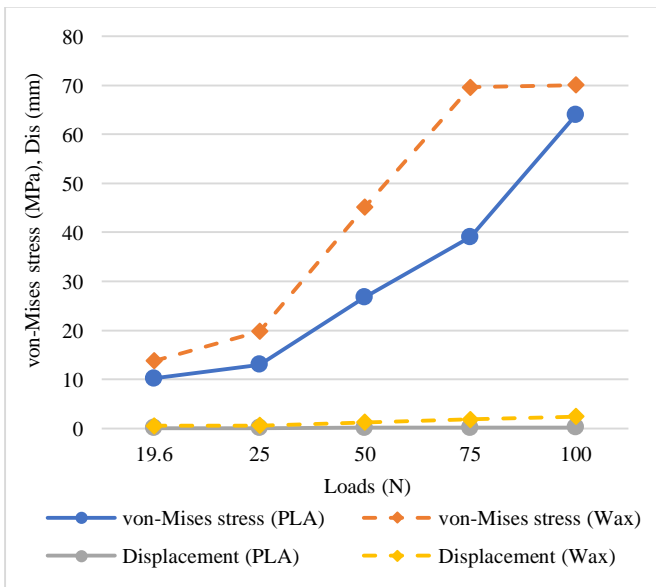


Fig. 14 Von-mises stress and displacement vs Compressive load for design 2

**Table 5. Compressive strength analysis on design 2**

Loads (N)	von-Mises stress (MPa)		Displacement (mm)	
	PLA	Wax	PLA	Wax
19.6	10.202	13.732	0.034	0.471
25	13.013	19.748	0.043	0.597
50	26.787	45.215	0.085	1.197
75	39.043	69.604	0.13	1.794
100	63.911	70.082	0.173	2.402

Table 5 and Figure 14 illustrate the changes in von-Mises stress and displacement for Design 2 under compressive load from 19.6 N to 100 N. von-Mises stress in PLA and castable wax resin material show similar trends. With increasing load, stress is seen to rise gradually in PLA material, whereas it increases proportionally in the wax material. However, constant stress is observed from 75 N to 100 N in wax material. The maximum equivalent von-Mises stress at 100 N load is 63.911 MPa for PLA and 70.082 MPa for castable wax resin. This comparison shows that wax can withstand significantly higher stress levels than PLA under identical loading conditions because it exceeds its yield strength.

The displacement in PLA and wax materials both exhibit an increase in displacement values with increasing load. Comparatively, the wax material model demonstrates more displacement, suggesting greater flexibility or deformation under stress. The comparison of PLA and castable wax resin material models under compressive loading conditions reveals distinct mechanical behaviors. Wax exhibits higher maximum von-Mises stress and displacement, indicating greater deformation under compression.

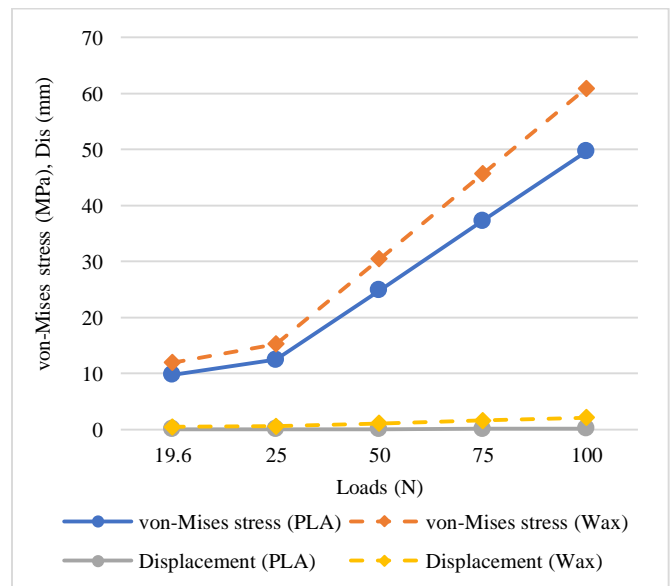


Fig.15 Von-mises stress and displacement vs Tensile load for Design 3



**Table 6. Tensile strength analysis on design 3**

Loads (N)	von-Mises stress (MPa)		Displacement (mm)	
	PLA	Wax	PLA	Wax
19.6	9.737	11.937	0.023	0.415
25	12.42	15.225	0.029	0.529
50	24.84	30.451	0.058	1.059
75	37.261	45.677	0.088	1.588
100	49.681	60.903	0.121	2.117

Table 6 and Figure 15 illustrate the changes in von-Mises stress and displacement for Design 3 under increasing tensile load from 19.6 N to 100 N. Both PLA and castable wax materials exhibit distinct patterns as the applied load. von-Mises stress is seen to increase with the applied load in PLA material with a maximum of 49.681 MPa at 100 N load.

The castable wax material shows a consistent increase in von-Mises stress proportional to the applied load, resulting in a higher maximum stress of 60.903 MPa at 100 N. This implies that both the PLA and wax materials have a more linear stress response to increasing loads. Displacement in PLA and castable wax materials is seen to increase with increasing load, specifically, maximum displacement at 100 N load and minimum displacement at 19.6 N load.

Castable wax material has higher maximum von-Mises stress and displacement, indicating greater deformation under tension. These findings emphasize the importance of considering material properties like stress tolerances and deformation characteristics when choosing between PLA and wax for applications involving tensile loads.

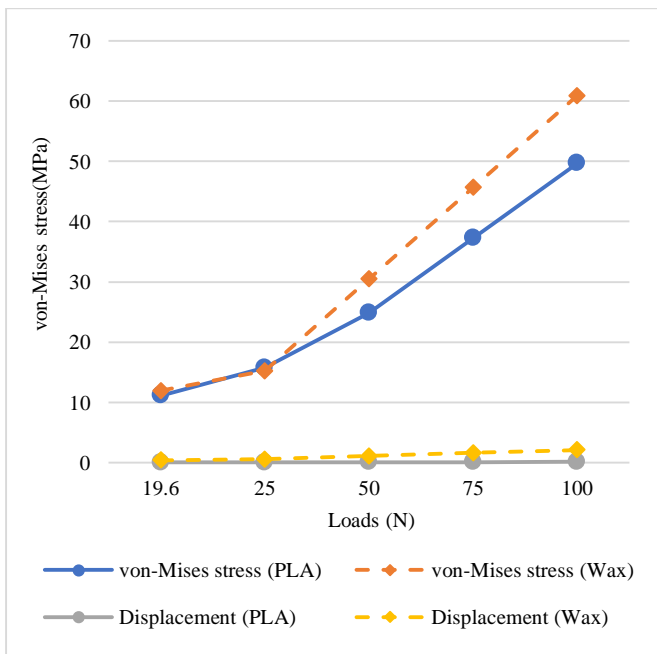


**Fig. 16 Von-mises stress and displacement vs Compressive load for design 3**

**Table 7. Compressive strength analysis on design 3**

Loads (N)	von-Mises stress (MPa)		Displacement (mm)	
	PLA	Wax	PLA	Wax
19.6	11.115	11.934	0.023	0.415
25	15.75	15.223	0.03	0.529
50	24.838	30.449	0.058	1.059
75	37.259	45.675	0.088	1.588
100	49.679	60.90	0.117	2.117

Table 7 and Figure 16 illustrate the changes in von-Mises stress and displacement for Design 3 under increasing compressive load from 19.6 N to 100 N. von-Mises stress in PLA and castable wax resin materials are seen to increase with the applied load. Both material exhibits increasing stress trends. PLA material shows a maximum equivalent von-Mises stress of 49.679 MPa at 100 N load, while the wax material demonstrates a higher maximum stress of 60.90 MPa under the same 100 N load condition. This difference suggests that wax can withstand higher stress levels than PLA under similar loading conditions. These results underscore the distinct mechanical properties of PLA and wax materials. Maximum and minimum displacement are seen at 100 N and 19.6 N, respectively, for both PLA and castable wax materials. When compressive load is induced, the castable wax material shows higher maximum von-Mises stress and displacement in contrast to the PLA material. This suggests that castable wax resin material can withstand greater stress levels.

A detailed analysis of the CAD model cufflink designs is executed, and the results are presented in the subsequent tables and graphs in Appendix 4. Appendices 4.1, 4.2, and 4.3 present the analysis results of von-Mises Stress vs Strain (tensile and compressive load) carried out on Design 1 (Oval base), Design 2 (Cross base) and Design 3 (Hexagonal base), respectively.

Appendix 4.1, Table 8 and Figure 17 show the changes in von-Mises stress and strain for Design 1 under increasing tensile load from 19.6 N to 100 N. Table 8 and Figure 17 illustrate a relationship between von-Mises stress (in MPa) and strain for two different materials (PLA and Castable wax resin), each represented by distinct markers and line styles. PLA material, depicted by a blue solid line with circular markers, shows a rapid increase in stress with a small increase in strain, indicating a steep and possibly brittle response. The stress rises from 11.106 MPa at a strain of 0.005 under a load of 19.6 N to 56.664 MPa at a strain of 0.028 under a load of 100 N. This indicates that the material experiences relatively low strain for significant increases in stress, suggesting stiffer and more brittle behavior. In contrast, the Castable wax material, shown by an orange dashed line with square markers, exhibits a more gradual increase in stress. This response suggests a more ductile material behavior, with the stress starting at 7.086 MPa at a

strain of 0.045 for the initial 19.6 N load and reaching 40.755 MPa at a strain of 0.253 for the highest load of 100 N. This suggests that Wax can undergo more strain before experiencing high stress, indicating a more ductile nature.

Table 9 and Figure 18 show the changes in von-Mises stress and strain for Design 1 under increasing compressive load from 19.6 N to 100 N. Under a load of 19.6 N, PLA experiences a von-Mises stress of 11.04 MPa at a strain of 0.005. As the load increases to 100 N, the von-Mises stress increases to 56.662 MPa, with a corresponding strain of 0.028. This sharp increase in stress with minimal strain indicates that PLA is a relatively brittle material with limited capacity for deformation under compressive loads. On the other side, Wax shows a more gradual increase in von-Mises stress with greater strain. At 19.6 N, the von-Mises stress for Wax is 7.805 MPa at a strain of 0.045. When the load reaches 100 N, the von-Mises stress is 39.825 MPa, with a corresponding strain of 0.231. The higher strain values compared to PLA indicate that Wax is more ductile and can sustain greater deformation before failure. In the von-Mises stress versus strain for both PLA and Wax, the PLA shows a steep rise in stress for minimal strain, indicating brittleness, while Wax demonstrates a more gradual increase in stress with higher strain, suggesting ductility.

Appendix 4.2, Table 10 and Figure 19 show the changes in von-Mises stress and strain for Design 2 under increasing tensile load from 19.6 N to 100 N. Table 10 and Figure 19 show the von-Mises stress and strain for Design 2, evaluated under varying loads for two materials, PLA and Wax. The values highlight distinct mechanical responses for each material when subjected to increasing tensile loads. For PLA material, the von-Mises stress starts at 10.204 MPa with a strain of 0.005 under a 19.6 N load. As the load increases to 100 N, the von-Mises stress reaches 52.061 MPa with a corresponding strain of 0.025. This behavior is consistent with a material that is relatively stiff and exhibits low strain under higher stress, which is characteristic of brittle materials. On the other hand, Wax exhibits a different mechanical behavior from PLA.

Under the initial load of 19.6 N, the von-Mises stress for Wax is significantly higher at 17.694 MPa, with a strain of 0.101. As the load increases, the von-mises stress peaks at 70.087 MPa under a load of 100 N, with a corresponding strain of 0.389. the higher strain values and the relatively large increase in stress suggest that Wax is more ductile and capable of undergoing substantial deformation before failure. The PLA curve demonstrates a steep increase in stress with minimal strain, reflecting its brittle nature. In contrast, Wax shows a much more gradual increase in stress with significantly higher strain, emphasizing its ductile nature and ability to accommodate more deformation under tensile loads.

Table 11 and Figure 20 show the changes in von-Mises stress and strain for Design 2 under increasing compressive load from 19.6 N to 100 N. The von-Mises stress for PLA begins at 10.202 MPa with a strain of 0.005 under a 19.6 N load. As the load increases to 100 N, the von-Mises stress to 63.911 MPa, with a strain of 0.023. This indicates that PLA exhibits a sharp increase in stress with relatively low strain, which is characteristic of brittle material with limited deformation capabilities. On the other hand, Wax shows a different mechanical behavior from PLA. Under the initial load of 19.6 N, the von-Mises stress for Wax is 13.732 MPa with a strain of 0.076. As the load increases to 100 N, the von-Mises stress reaches 70.082 MPa, with a corresponding strain of 0.389. the higher strain values and more gradual increase in stress indicate that Wax is more ductile, allowing for greater deformation under compressive forces. The curve for PLA material shows a steep rise in stress with low strain, reflecting its brittle nature. On the other side, the Wax curve exhibits a more gradual stress increase with significantly higher strain, indicating its ductility to undergo more deformation before reaching its stress limit.

Appendix 4.3, Table 12 and Figure 21 show the changes in von-Mises stress and strain for Design 3 under increasing tensile load from 19.6 N to 100 N. Table 11 and Figure 21 provide the von-Mises stress and strain values for Design 3, evaluated under the different loads ranging from 19.6 N to 100 N for two materials, PLA and Wax. For PLA, the von-Mises stress rises to 49.681 MPa, with a corresponding strain of 0.022. PLA exhibits a characteristic sharp increase in stress with relatively low strain, indicating that the material is stiff and brittle, with limited capacity for deformation under tensile loads. For Wax under the initial load of 19.6 N, Wax experiences a von-Mises stress of 11.937 MPa, with a strain of 0.054. As the load increases to 100 N, the von-Mises stress reaches 60.903 MPa, with a corresponding strain of 0.278. the higher strain values indicate that Wax can accommodate more deformation under tensile forces. The PLA curve shows a steep increase in stress with minimal strain, consistent with brittle behavior, while the Wax curve displays a more gradual increase in stress with higher strain, illustrating its ductile properties and greater deformation capacity under load.

Table 13 and Figure 22 show the changes in von-Mises stress and strain for Design 3 under increasing compressive load from 19.6 N to 100 N. For PLA, as the load increases from 19.6 N to 100 N, the von-Mises stress increases from 11.115 MPa to 49.679 MPa, with corresponding values from 0.005 to 0.023. similarly, for Wax, the von-Mises stress shows an increase from 11.934 MPa at 19.6 N to 60.9 MPa at 100 N, with strain values increasing from 0.054 to 0.278. The graph demonstrates a linear relationship between stress and strain for both materials, with Wax showing a higher strain than PLA at equivalent stress levels. This indicates that Wax is more deformable under stress compared to PLA,

which aligns with the higher strain values observed for Wax at each corresponding load.

### 3.2. 3D Printing of Cowrie Shell-Inspired Cufflink

According to the analytical results, it is observed that castable wax resin material has a higher von-Mises stress but is within the limit as compared to that of PLA material. There is minimal displacement in both materials, with wax showing slightly more displacement and PLA showing negligible displacement. Consequently, castable wax resin material is selected for 3D printing of the cowrie shell-inspired jewellery designs due to its widespread use in conventional jewellery making. SLA printing technology is capable of printing castable wax resin material; hence, it is used in this work. Table 14 exhibits the parameters of the 3D printing process.

**Table 14. Printing variables for wax material**

Parameters	Values
Material type	Castable wax resin
Layer height (mm)	0.05
Number of shells	2
Exposure time (sec)	14
Build time (hr, min)	3, 15
Support structure	Linear/Cone

SLA printing is performed on the Elegoo Saturn 2 8K 3D printer, which has a build volume of 219 mm x 123 mm x 250 mm. 3D printer and UV curing machines are illustrated in Figure 23. Chitubox V1.9.6 software is used to specify the parameters and slicing purposes, and the support structures are depicted in Figure 24. TLP resin is utilized to create cowrie shell-inspired cufflinks. Visual reference of the 3D printed cufflinks is exhibited in Figure 25, which shows the nature-inspired cowrie shell on the cufflinks.



**Fig. 23 SLA-based 3D printer and UV curing machine**

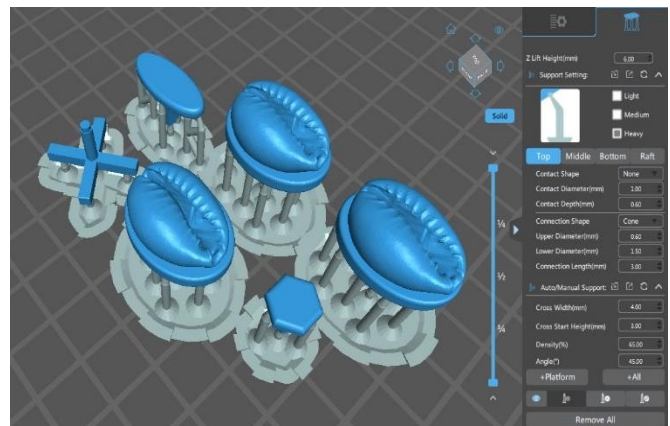


**Fig. 24 Support structures creation in Chitubox V1.9.6 software**





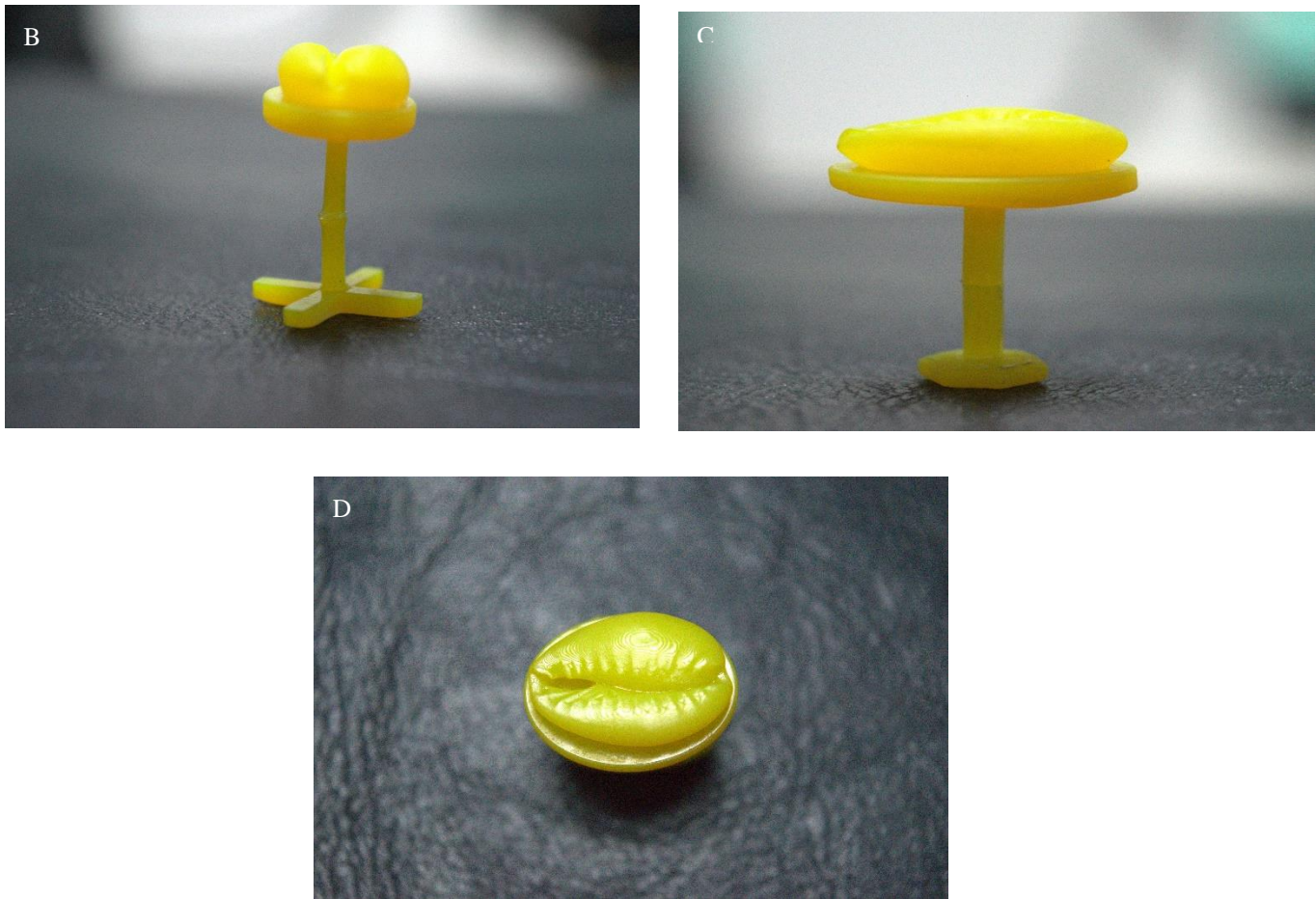


Fig. 25 3D printed cowrie shell-inspired Cufflink with castable wax material (A) Cufflink design 1, (B) Cufflink design 2, (C) Cufflink design 3, and (D) Nature-inspired cowrie shell in cufflink.

#### 4. Conclusion

This work presents the significance of 3D printing in the design and development of unique nature-inspired jewellery. Cowrie shells that are found abundantly near seashores have been selected as the nature-inspired form for designing cufflink jewellery using the QFD tool. To showcase the ease of modelling complex and intricate geometries, the cowrie shell is 3D scanned and then used for CAD modelling of three conceptual designs with oval, cross, and hexagonal base structures. Analytical results based on tensile and compressive loading on the models with PLA and castable wax resin materials at various loading conditions indicate

that castable wax resin is the appropriate material for 3D printing. Three cowrie shell-inspired cufflink designs are then 3D printed successfully using castable wax resin material on an SLA printer. The approach presented here showcases the advantages of 3D printing in the ease of modelling complex shapes with less time and wastage in the jewellery manufacturing industry.

#### Acknowledgments

Author 1, Author 2, and Author 3 contributed equally to this work.



## References

- [1] Noor Adila Mohd Rajili et al., "Processes, Methods and Knowledge Creation in Jewellery Design Practice," *ICoRD'15-Research into Design across Boundaries*, vol. 1, pp. 303-313, 2015. [[CrossRef](#)] [[Google Scholar](#)] [[Publisher Link](#)]
- [2] Cecilia Lico, "Applying 3D Modelling Technology to Traditional Craftwork: Rapid Prototyping in Artisanal Jewellery Making and Its Impact on the Perceived Value of Jewellery," Thesis, Faculty of Planning, University of Montreal, Canada, pp. 1-161, 2015. [[Google Scholar](#)] [[Publisher Link](#)]
- [3] Athanasios Manavis et al., "Jewellery Design and Wearable Applications: A Design Thinking Approach," *International Symposium on Graphic Engineering and Design*, pp. 591-596, 2020. [[CrossRef](#)] [[Google Scholar](#)] [[Publisher Link](#)]
- [4] Wendy Yothers, and Resmi Gangadharan, "Narration on Ethnic Jewellery of Kerala-Focusing on Design, Inspiration and Morphology of Motifs," *Journal of Textile Engineering & Fashion Technology*, vol. 6, no. 6, pp.267-274, 2020. [[CrossRef](#)] [[Google Scholar](#)] [[Publisher Link](#)]
- [5] Hongxia Chu, "Research on 3D Jewelry Design Based on Virtual Reality Technology," *Wireless Communications and Mobile Computing*, vol. 2022, no. 1, pp. 1-9, 2022. [[CrossRef](#)] [[Google Scholar](#)] [[Publisher Link](#)]
- [6] Hira Das Akash, "Additive Manufacturing in the Jewelry Industry-Design and Production," M.E. Thesis, Grant Tallinn University of Technology (Taltech), Tallinn, Estonia, 2021. [[Publisher Link](#)]
- [7] Cufflink, Wikipedia. [Online]. Available: <https://en.wikipedia.org/wiki/Cufflink>
- [8] Kim Bui, Cufflinks 101: A Gentlemen's Introduction to Cufflinks. [Online]. Available: <https://journal.fredfloris.eu/cufflinks-101-a-gentlemens-introduction-to-cufflinks>
- [9] The Tateossian Guide to Different Types of Cufflink, 2023. [Online]. Available: <https://us.tateossian.com/community/blog/the-tateossian-guide-to-different-types-of-cufflink>
- [10] Silvia Giacomini, "Additive Manufacturing in the Goldsmith Industry. Technological Issues, Economic Benefits and Firms' Actual Adoption," Master's Thesis, Polytechnic University of Turin, Italy, 2020. [[CrossRef](#)] [[Google Scholar](#)] [[Publisher Link](#)]
- [11] Nosheen Fatma et al., "Prospects of Jewelry Designing and Production by Additive Manufacturing," *Current Advances in Mechanical Engineering: Select Proceedings of ICRAMERD*, pp. 869-879, 2021. [[CrossRef](#)] [[Google Scholar](#)] [[Publisher Link](#)]
- [12] Silvia Giacomini, "3D-Printed Jewelry-A New Era for Online Jewelry Customization (Exploring Consumer Perceptions, Consumption Drivers and Barriers for the Portuguese Online Market)," Thesis, Catholic University of Portugal, Lisbon, Portugal, 2022. [[Google Scholar](#)] [[Publisher Link](#)]
- [13] Natalija Budinski et al., "Interconnection of Materials Science, 3D Printing and Mathematic in Interdisciplinary Education," *Sted Journal*, vol. 1, no. 2, pp. 21-30, 2019. [[Google Scholar](#)] [[Publisher Link](#)]
- [14] Mohamed Selim Korium et al., "Direct Metal Laser Sintering of Precious Metals for Jewelry Applications: Process Parameter Selection and Microstructure Analysis," *IEEE Access*, vol. 9, pp. 126530-126540, 2021. [[CrossRef](#)] [[Google Scholar](#)] [[Publisher Link](#)]
- [15] Priya Thakur, "Floral Jewellery in Ancient Indian Tradition," *SAARC Culture*, vol. 6, pp. 79-87, 2018. [[Google Scholar](#)] [[Publisher Link](#)]
- [16] Vaia Tzintzi et al., "Conceptual Design of Jewellery: A Space-Based Aesthetics Approach," *MATEC Web of Conferences*, EDP Sciences, vol. 112, pp. 1-6, 2017. [[CrossRef](#)] [[Google Scholar](#)] [[Publisher Link](#)]
- [17] Betül Çitir, Ufuk Cebeci, and Özgenur Tuncer, "Application of Quality Function Deployment with Different Consumer Behavior of Generations in Jewelry Sector," *Journal of Current Research on Engineering, Technology*, vol. 7, no. 1, pp. 75-92, 2021. [[CrossRef](#)] [[Google Scholar](#)] [[Publisher Link](#)]
- [18] Vira Bublyk, "Jewelry Inspired by Flowers Creating Jewelry with A Modern Flower Image," Master thesis, Telemark University College, Porsgrunn, Telemark, Norway, 2014. [[Google Scholar](#)] [[Publisher Link](#)]
- [19] Karin Košak et al., "3D Printed Jewellery Design Process Based on Sculpture Inspiration," *International Symposium on Graphic Engineering and Design*, pp. 507-514, 2020. [[CrossRef](#)] [[Google Scholar](#)] [[Publisher Link](#)]
- [20] Michaela T. Espino et al., "Statistical Methods for Design and Testing of 3D-Printed Polymers," *MRS Communications*, vol. 13, no. 2, pp. 193-211, 2023. [[CrossRef](#)] [[Google Scholar](#)] [[Publisher Link](#)]
- [21] Y. Ling Yap, and W.Y. Yeong, "Additive Manufacture of Fashion and Jewellery Products: A Mini Review," *Virtual and Physical Prototyping*, vol. 9, no. 3, pp. 195-201, 2014. [[CrossRef](#)] [[Google Scholar](#)] [[Publisher Link](#)]
- [22] Anupama Pasricha, and Rachel Greeninger, "Exploration of 3D Printing to Create Zero-Waste Sustainable Fashion Notions and Jewelry," *Fashion and Textiles*, vol. 5, no. 1, pp. 1-18, 2018. [[CrossRef](#)] [[Google Scholar](#)] [[Publisher Link](#)]
- [23] Telma Ferreira et al., "Additive Manufacturing in Jewellery Design," *ASME 2012 11<sup>th</sup> Biennial Conference on Engineering Systems Design and Analysis*, vol. 4, pp. 187-194, 2012. [[CrossRef](#)] [[Google Scholar](#)] [[Publisher Link](#)]
- [24] Frank Cooper, "Sintering and Additive Manufacturing: 'Additive Manufacturing and the New Paradigm for the Jewellery Manufacturer,'" *Progress in Additive Manufacturing*, vol. 1, no. 1-2, pp. 29-43, 2016. [[CrossRef](#)] [[Google Scholar](#)] [[Publisher Link](#)]

[25] Diego Matricano, and Giorgio Vitagliano, “International Marketing Strategies in The Jewellery Industry: Are They Standardized, Adapted or Both?,” *International Journal of Marketing Studies*, vol. 10, no. 1, pp.1-10, 2018. [[CrossRef](#)] [[Google Scholar](#)] [[Publisher Link](#)]

[26] Ivan Emeka Okonkwo, “The Product Categories, Challenges, and Prospects of Handicraft Production in Nigeria,” *IGWEBUIKE: African Journal of Arts and Humanities*, vol. 3, no. 5, pp. 133-157, 2017. [[Google Scholar](#)] [[Publisher Link](#)]

[27] Paola Garbagnoli et al., “Innovative Processes for Jewellery Production,” *A Matter of Design Making Society through Science and Technology*, pp. 341-349, 2014. [[Google Scholar](#)] [[Publisher Link](#)]

[28] Hirpa Gelgele Lemu, and Robin H. Helle, “A Case Study on Use of 3D Scanning for Reverse Engineering and Quality Control,” *Materials Today: Proceedings*, vol. 45, pp. 5255-5262, 2021. [[CrossRef](#)] [[Google Scholar](#)] [[Publisher Link](#)]

[29] Alessandro Brun, and Parisa Sepahvani, “Influences of Additive Manufacturing (3d Printers) on The Production Cost and Future of Jewelry Industry,” Thesis, Politecnico Di Milano, Italy, 2015. [[Google Scholar](#)] [[Publisher Link](#)]

[30] Mohamed Korium, “Development of a Metal 3D Printing Process for Jewelry Production Utilizing Titanium,” M.E. Thesis, Lappeenranta-Lahti University of Technology (LUT), Lappeenranta, Finland, 2019. [[Google Scholar](#)] [[Publisher Link](#)]

### Appendix 1 QFD of Cufflink

Category	Types of Inspired Items	Availability of the Inspired Item	Shape/Form of the Inspired Item	Cost of the Inspired Item	Size of the Inspired Item
Sea Shells	Univalves	☑	×	×	☑
	Bivalvia	☑	✓	✓	✓
	Monoplacophor	—	✓	×	☑
	Cowrie shell	✓	✓	✓	✓
Flowers	African Daisy	✓	☑	✓	✓
	Snapdragon	✓	×	✓	☑
	Balsam	✓	×	✓	✓
	Lavender	×	✓	×	☑
	Marigold	✓	✓	✓	✓
Fruits	Mango	✓	☑	✓	✓
	Lemon	✓	☑	✓	✓
	Kiwi	✓	×	✓	✓
	Papaya	✓	☑	✓	×
	Peaches	☑	☑	✓	×
	Rambutan	☑	×	✓	✓
	Raspberries	✓	☑	☑	✓
	Jack Fruit	✓	×	✓	×
	Dragon Fruit	✓	☑	✓	☑
	Custard apples	✓	☑	✓	×
	Kaffir lime	✓	×	✓	×
	Ugli Fruit	✓	×	✓	☑
Plants	Boston Fern	☑	×	✓	✓
	Creeper Plant	☑	×	✓	☑
	ZZ plant	✓	×	✓	☑
	Prayer	✓	×	☑	×
	Anthurium	✓	☑	☑	✓
	Aquatic	✓	×	✓	☑
	Shrubs	✓	×	✓	☑
	Jade	✓	×	✓	✓
	Peace Lilly	✓	☑	✓	✓
	Chinese Money Plant	✓	×	✓	✓
	Begonia	✓	×	✓	☑
	Asparagus Fem	✓	×	✓	×
Kalanchoe	✓	×	✓	×	

	Echeveria	✓	☑	✓	✓
	Lithops	✓	×	☑	☑
	Oxalis	☑	×	✓	✓
	Polka dot	✓	☑	✓	☑

**Appendix 2 Assessment of Parameters based on QFD**

Inspired Model Category	Types	Cufflinks		
		✓	☑	×
<b>Sea shells</b>	Univalves	0	2	2
	Bivalvia	3	1	0
	Monoplacophor	1	1	1
	Cowrie shell	4	0	0
<b>Flowers</b>	African Daisy	3	1	0
	Snapdragon	2	1	0
	Balsam	3	0	1
	Lavender	1	1	2
	Marigold	4	0	0
<b>Fruits</b>	Mango	3	1	0
	Lemon	3	1	0
	Kiwi	3	0	1
	Papaya	2	1	1
	Peaches	1	2	1
	Rambutan	2	1	1
	Raspberries	2	2	0
	Jack Fruit	2	0	2
	Dragon Fruit	2	2	0
	Custard apples	2	1	1
	Kaffir lime	2	0	2
	Ugli Fruit	2	1	1
<b>Plants</b>	Boston Fern	2	1	1
	Creeper Plant	1	2	1
	ZZ plant	2	1	1
	Prayer	2	0	2
	Anthurium	2	2	0
	Aquatic	2	1	1
	Shrubs	2	1	1
	Jade	3	0	1
	Peace Lilly	3	1	0
	Chinese Money Plant	3	0	1
	Begonia	2	1	1
	Asparagus Fem	2	0	2
	Kalanchoe	2	0	2
	Echeveria	3	1	0
	Lithops	1	2	1
	Oxalis	2	1	1
	Polka dot	2	2	0

**Appendix 3 Analysis Results**

**3.1. Tensile Test Analysis Results of Design 1 (Oval base)**

Material / Loads	Parameters	19.6 N	25 N	50 N	75 N	100 N
PLA	Von-Mises stress (MPa)					
	Displacement (mm)					
	Strain					
Castable Wax Resin	Von-Mises stress (MPa)					
	Displacement (mm)					
	Strain					



**Compressive Test Analysis Results of Design 1 (Oval base)**

Material / Loads	Parameters	19.6 N	25 N	50 N	75 N	100 N
PLA	Von-Mises stress (MPa)					
	Displacement (mm)					
	Strain					
Castable Wax Resin	Von-Mises stress (MPa)					
	Displacement (mm)					
	Strain					

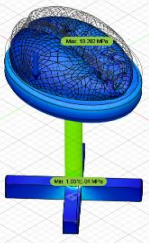
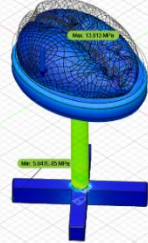
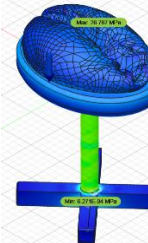
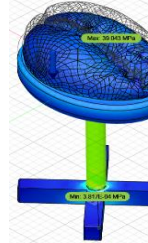
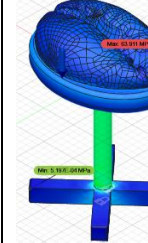
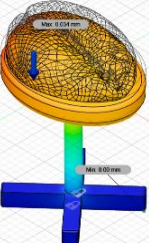
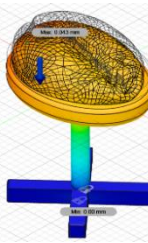
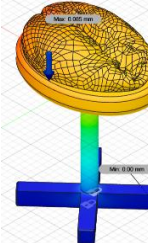
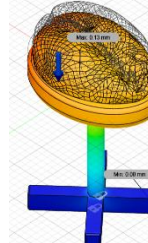
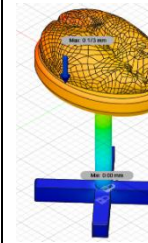
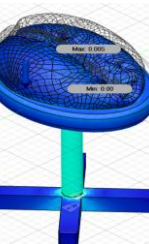
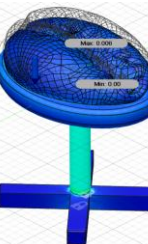
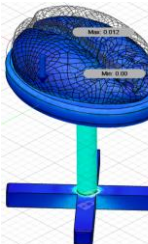
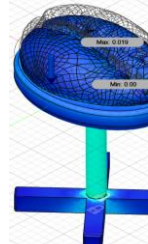
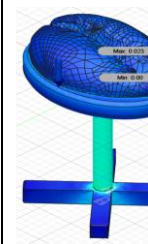
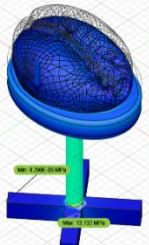
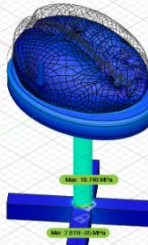
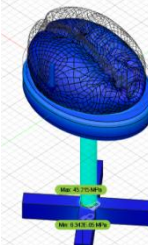
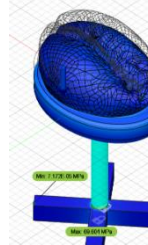
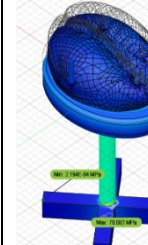
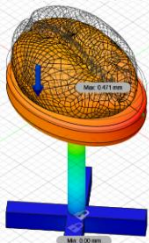
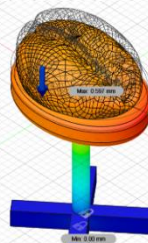
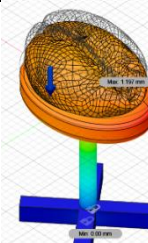
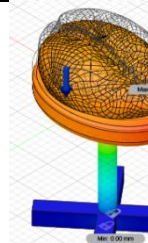
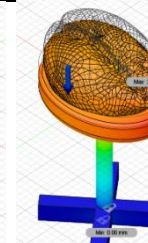
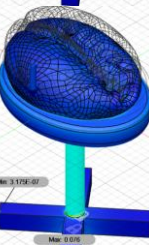
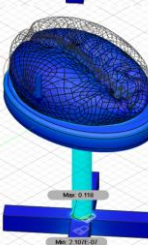
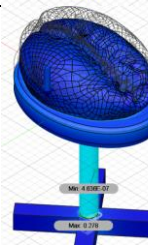
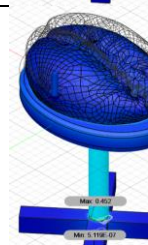
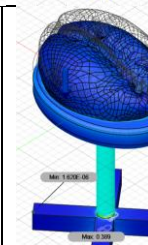


3.2. Tensile Test Analysis Results of Design 2 (Cross base)

Material / Loads	Parameters	19.6 N	25 N	50 N	75 N	100 N
PLA	Von-Mises stress (MPa)					
	Displacement (mm)					
	Strain					
Castable Wax Resin	Von-Mises stress (MPa)					
	Displacement (mm)					
	Strain					

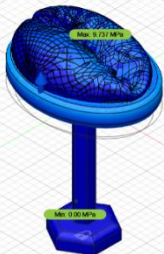
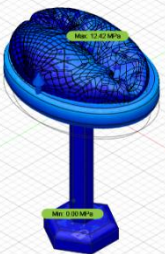
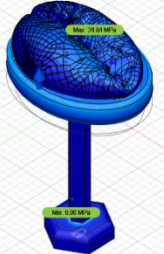
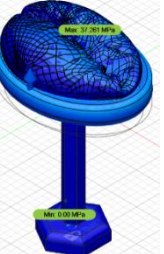
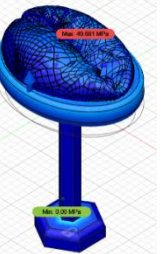
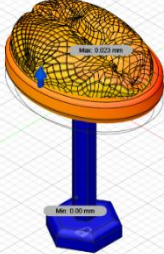
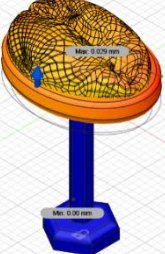
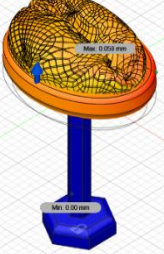
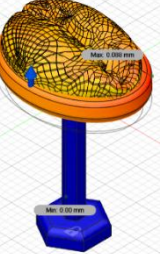
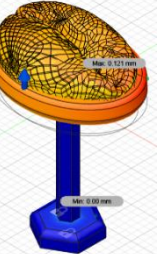
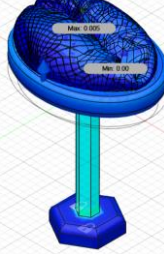
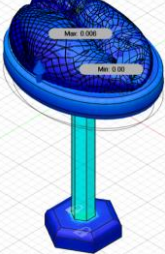
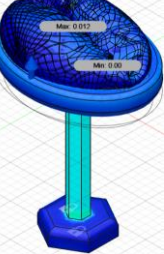
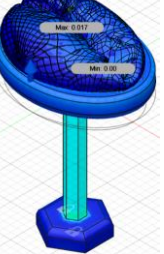
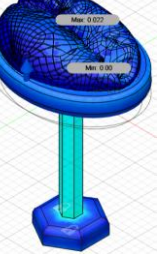
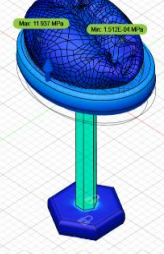
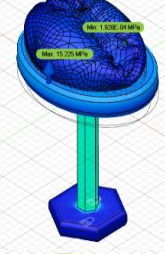
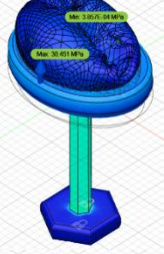
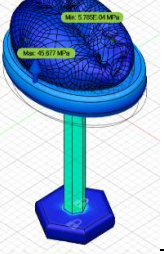
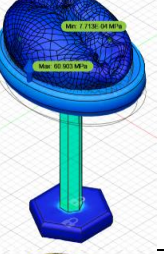
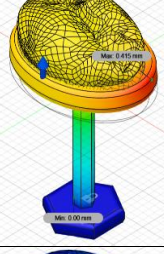
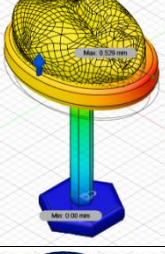
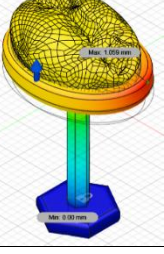
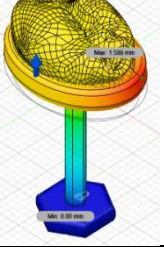
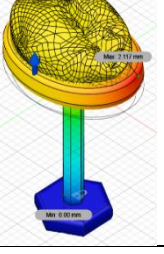
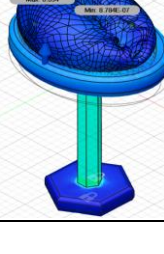
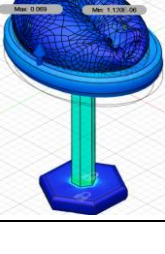
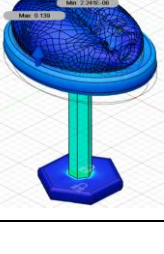
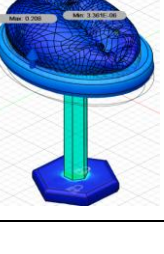
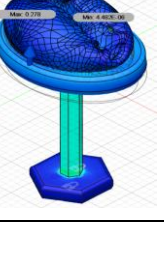


**Compressive Test Analysis Results of Design 2 (Cross base)**

Material / Loads	Parameters	19.6 N	25 N	50 N	75 N	100 N
PLA	Von-Mises stress (MPa)					
	Displacement (mm)					
	Strain					
Castable Wax Resin	Von-Mises stress (MPa)					
	Displacement (mm)					
	Strain					

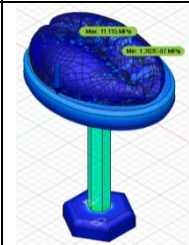
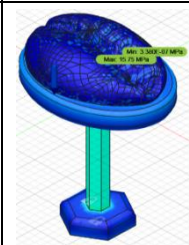
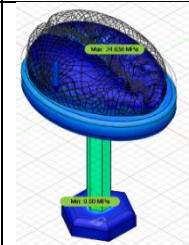
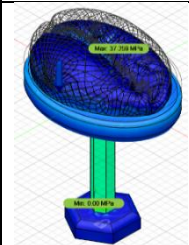
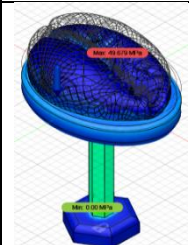
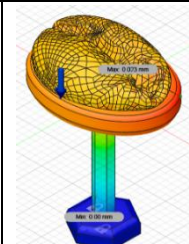
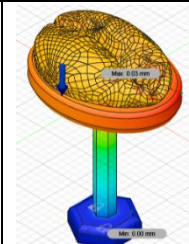
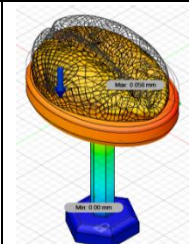
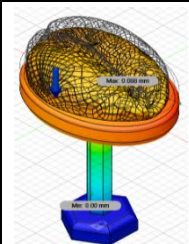
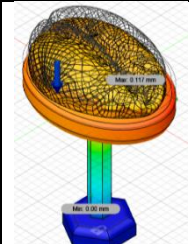
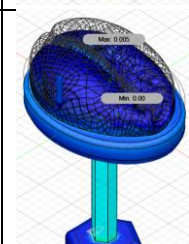
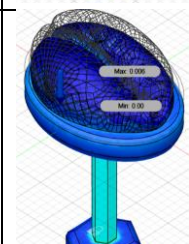
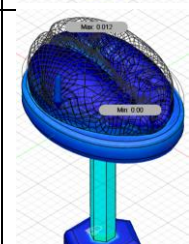
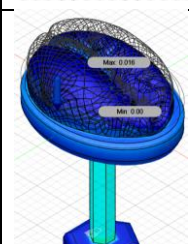
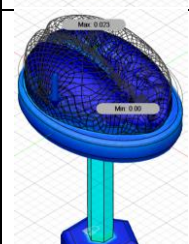
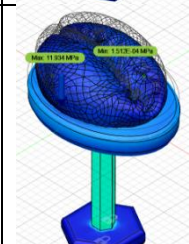
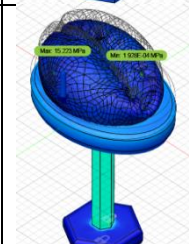
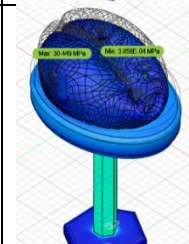
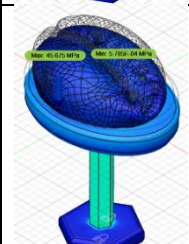
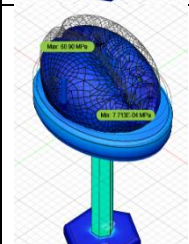
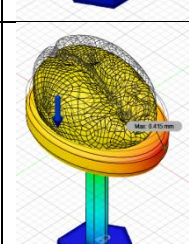
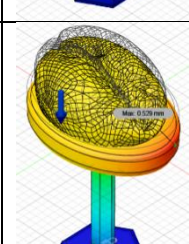
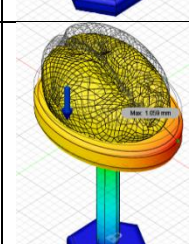
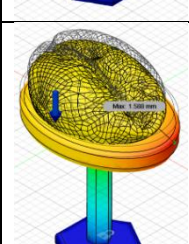
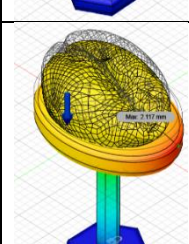
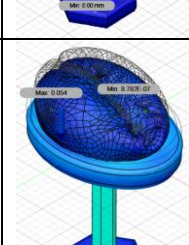
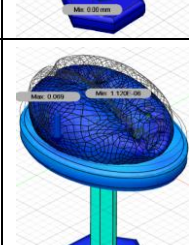
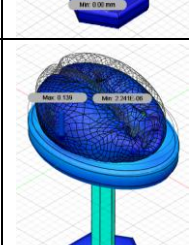
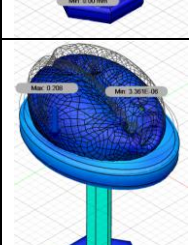
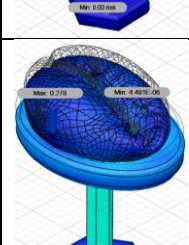


3.3. Tensile Test Analysis Results of Design 3 (Hexagonal base)

Material / Loads	Parameters	19.6 N	25 N	50 N	75 N	100 N
PLA	Von-Mises stress (MPa)					
	Displacement (mm)					
	Strain					
Castable Wax Resin	Von-Mises stress (MPa)					
	Displacement (mm)					
	Strain					



**Tensile Test Analysis Results of Design 3 (Hexagonal base)**

Material / Loads	Parameters	19.6 N	25 N	50 N	75 N	100 N
PLA	Von-Mises stress (MPa)					
	Displacement (mm)					
	Strain					
Castable Wax Resin	Von-Mises stress (MPa)					
	Displacement (mm)					
	Strain					

### Appendix 4 Analysis Results

#### 4.1. Von-Mises Stress vs Strain Analysis on Design 1 (Oval base)

##### 4.1.1. Tensile Strength Analysis

Table 8. Von-mises stress and stain analytical values for design 1

Loads (N)	Von-Mises Stress (MPa)		Strain	
	(PLA)	(Wax)	(PLA)	(Wax)
19.6	11.106	7.806	0.005	0.045
25	14.166	9.957	0.007	0.058
50	28.332	19.913	0.014	0.116
75	42.498	29.87	0.021	0.174
100	56.664	40.755	0.028	0.253

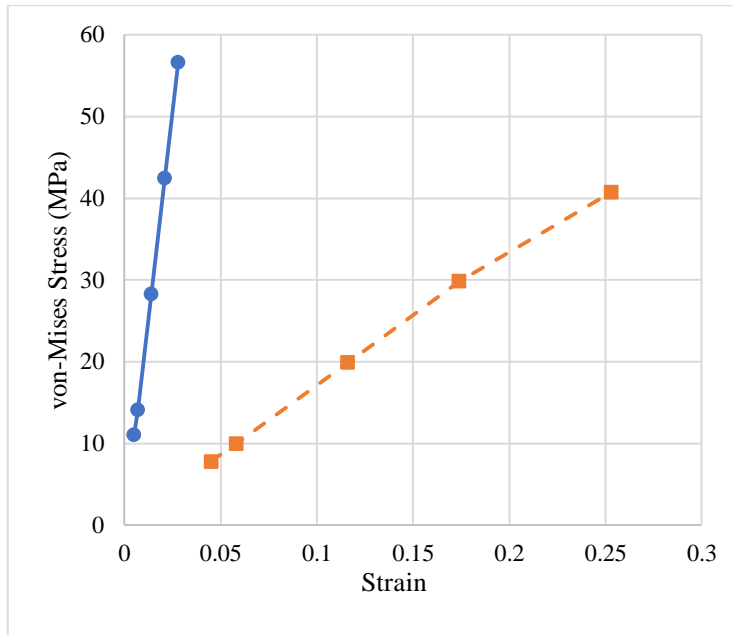


Fig. 17 Von-mises stress vs Strain graph for Design 1

##### 4.1.2. Compressive Strength Analysis

Table 9. Von-mises stress and stain analytical values for design 1

Loads (N)	Von-Mises stress (MPa)		Strain	
	(PLA)	(Wax)	(PLA)	(Wax)
19.6	11.04	7.805	0.005	0.045
25	14.164	9.955	0.007	0.058
50	28.329	19.912	0.014	0.116
75	42.496	29.869	0.021	0.174
100	56.662	39.825	0.028	0.231

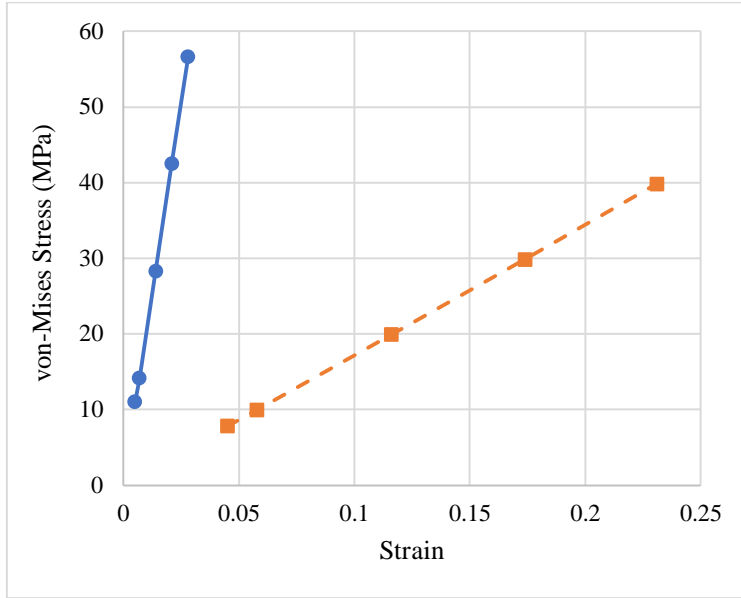


Fig. 18 Von-mises stress vs Strain graph for design 1

#### 4.2. Von-Mises Stress vs Strain Analysis on Design 2 (Cross base)

##### 4.2.1. Tensile Strength Analysis

Table 10. Von-mises stress and stain analytical values for design 2

Loads (N)	Von-Mises Stress (MPa)		Strain	
	(PLA)	(Wax)	(PLA)	(Wax)
19.6	10.204	17.694	0.005	0.101
25	13.015	17.521	0.006	0.097
50	26.03	43.658	0.012	0.261
75	39.045	67.835	0.019	0.418
100	52.061	70.087	0.025	0.389

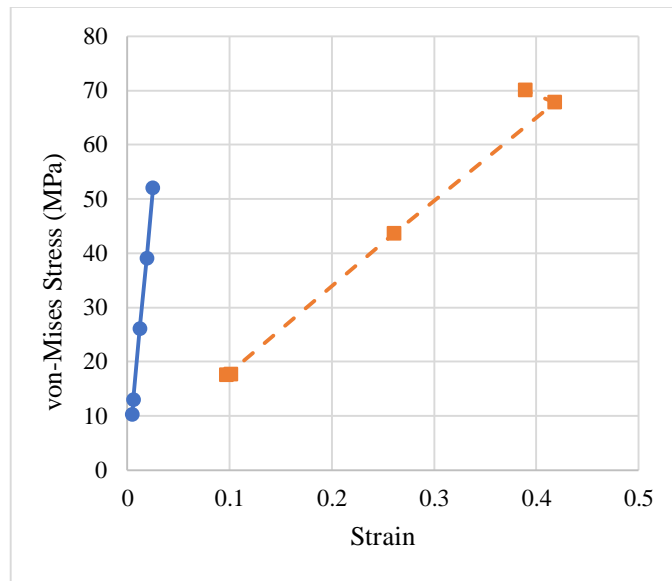


Fig. 19 Von-mises stress vs Strain graph for design 2

4.2.2. Compressive Strength Analysis

Table 11. Von-mises stress and stain analytical values for design 2

Loads (N)	von-Mises stress (MPa)		Strain	
	(PLA)	(Wax)	(PLA)	(Wax)
19.6	10.202	13.732	0.005	0.076
25	13.013	19.748	0.006	0.118
50	26.787	45.215	0.012	0.278
75	39.043	69.604	0.019	0.452
100	63.911	70.082	0.023	0.389

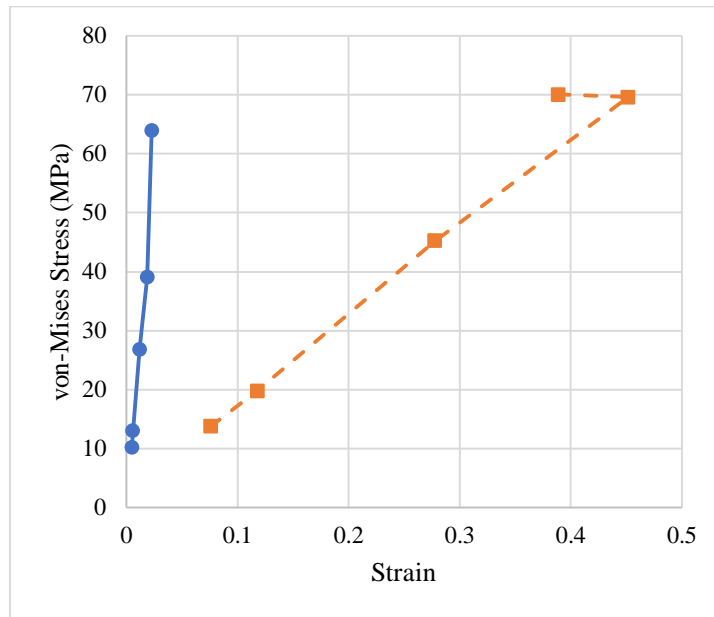


Fig. 20 Von-mises stress vs Strain graph for design 2

4.3. Von-Mises Stress vs Strain Analysis on Design 3 (Hexagonal base)

4.3.1. Tensile Strength Analysis

Table 12. Von-mises stress and stain analytical values for design 3

Loads (N)	von-Mises stress (MPa)		Strain	
	(PLA)	(Wax)	(PLA)	(Wax)
19.6	9.737	11.937	0.005	0.054
25	12.42	15.225	0.006	0.069
50	24.84	30.451	0.012	0.139
75	37.261	45.677	0.017	0.208
100	49.681	60.903	0.022	0.278



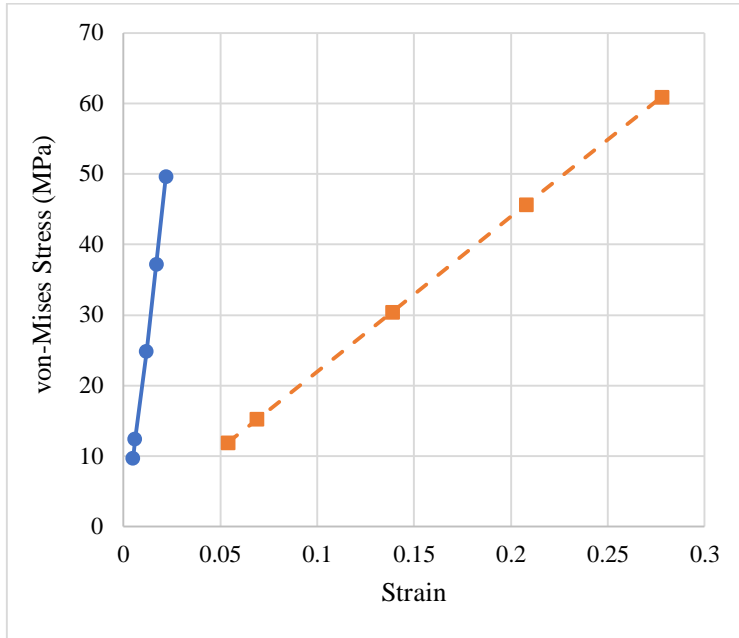


Fig. 21 Von-mises stress vs Strain graph for design 3

4.3.2. Compressive Strength Analysis

Table 13. Von-mises stress and stain analytical values for design 3

Loads (N)	von-Mises stress (MPa)		Strain	
	(PLA)	(Wax)	(PLA)	(Wax)
19.6	11.115	11.934	0.005	0.054
25	15.75	15.223	0.006	0.069
50	24.838	30.449	0.012	0.139
75	37.259	45.675	0.016	0.208
100	49.679	60.9	0.023	0.278

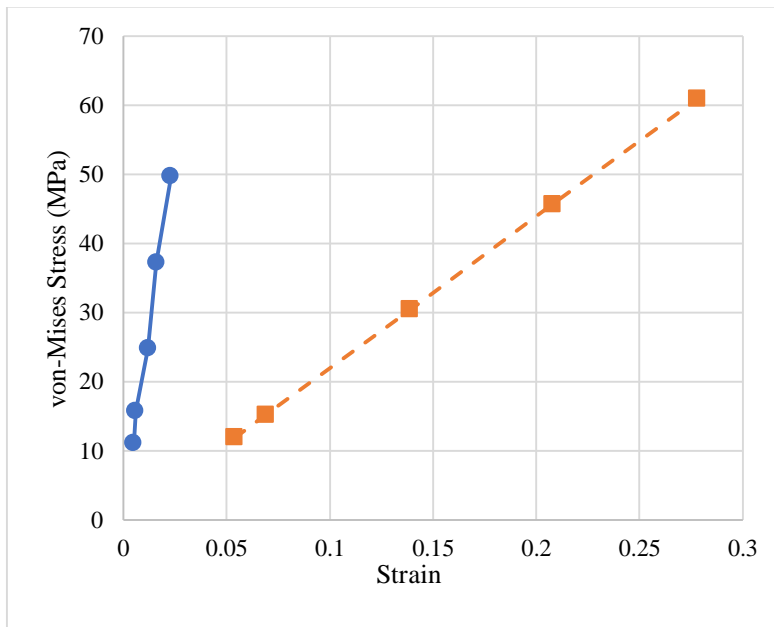


Fig. 22 Von-mises stress vs Strain graph for design 3